ChemComm

Accepted Manuscript

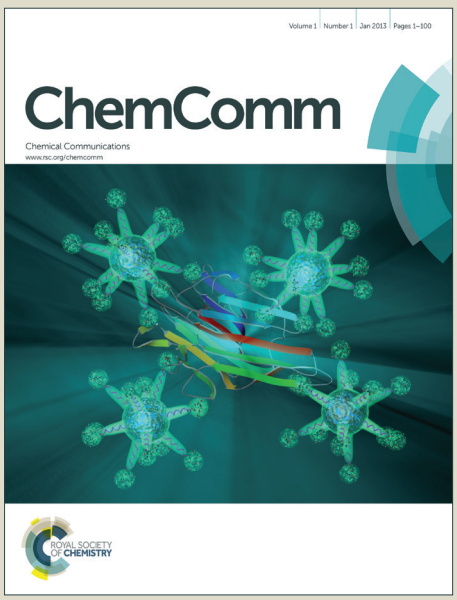

ROYAL SOCIETY OF CHEMISTRY

www.rsc.org/chemcomm

Journal Name

RSCPublishing

COMMUNICATION

Hollow nitrogen-doped carbon spheres as an efficient and durable electrocatalyst for oxygen reduction

Cite this: DOI: 10.1039/x0xx00000x

Jakkid Sanetuntikul [a], Tao Hang [b,*], and Sangaraju Shanmugam [a]*

Received 00th January 2014,
Accepted 00th January 2014

DOI: 10.1039/x0xx00000x

www.rsc.org/

Hollow nitrogen-doped carbon spheres (HNCS) were prepared by a facile method as non-precious catalyst for oxygen reduction reaction (ORR). The HNCS catalyst exhibited a comparable ORR activity with a commercial Pt/C catalyst and superior stability in alkaline electrolyte medium.

Proton exchange membrane fuel cells (PEMFCs) are extensively studied over the last two decades and still receiving tremendous interest as a promising power source for zero-emission electric vehicles due to their high-energy conversion efficiencies and low of air pollution[1]. Electrocatalyst plays an important role in driving the fuel cell reactions. It is generally practiced that Pt nanoparticles dispersed on high surface area carbon support (Pt/C) and Pt-alloy with transition metals are usually used as major catalyst for fuel cell. Still, Pt/C is the most effective catalyst for ORR. However, these catalysts imposed a number of disadvantages such as high cost, limited supply of Pt are the most technical limitations for the successful commercialization of fuel cell technology. Moreover, the poor ORR activity of Pt/C is also one of the major critical challenges for energy conversion efficiency PEMFCs[2,3]. Meanwhile, many new types of Pt-based catalysts have been synthesized and explored as the alternative catalyst to Pt/C and reduce the Pt content. The design of high-performance cathode catalyst is essential to reduce the catalysts cost, improve the ORR activity and durability. Thus, the fabrication of highly active and durable non-precious catalyst is definitely preferable and has turned into a great challenge for today's fuel cell research community[4,5]

Recently, nitrogen-doped carbon materials received tremendous importance as non-precious metal electrodes, due to the incorporation of nitrogen into carbon framework can create active sites for oxygen adsorption and reduction. Various nitrogen-doped on carbon including carbon nanotube (CNT)[6,7], multi-wall carbon nanotube (MWCNT)[8,9], mesoporous carbon[10], graphene[11,12] and metal organic framework (MOF)[13], have been explored as alternative catalysts to Pt/C. However, the ORR activities of N-doped carbons are still on less competitive compared to Pt. Therefore, the development of cost-effective and highly active ORR catalyst is required. Herein, we develop a simple and an easy method for the preparation of hollow nitrogen-doped carbon sphere (HNCS) and explored as a non-precious catalyst for ORR. The fabrication of HNCS was accomplished by a facile and cost-effective route using a dry-autoclaving of iron (III) diethylene triaminepentaacetate (Fe-DTPA) as a single precursor for carbon, nitrogen and iron. The reported method is a straight-forward, environmentally-friendly, highly re-producible and solvent-, catalyst-free and easy to handle. The synthesis was carried out by pyrolysing the precursor at 700 °C and 900 °C with a heating rate of 10 °C min^{-1} for 1 h under autogenic pressure resulted in Fe_3O_4 and Fe^0 filled in carbon spheres, respectively (Fig. S2-S4, ESI†). The as-synthesized products were stirred in concentrated HCl for 24 h at room temperature to remove the oxide core and the carbons derived from Fe_3O_4@C and Fe@C denoted as HNCS71 and HNCS91 (Scheme 1). The acid treated products were washed by copious water till pH of aliquots reach neutral, and then dried overnight in a vacuum oven.

Fig. 1(a-b) shows the SEM images of HNCS71 and HNCS91 reveal that after acid-treatment, the products show hollow sphere structure of carbon. The hollow sphere diameter is about 800 nm with a wall thickness of 100 nm and these spheres are free from oxide and metal core, which clearly evidenced by high-resolution TEM image (Fig.1 (c-d)). The X-ray diffraction patterns of HNCS71 and HNCS91 catalysts are shown in Fig. 2a. HNCS91 catalyst shows a strong and sharp peak at 27.1^0 (2θ) indicating the formation highly ordered carbon structure, which is due to the higher temperature pyrolysis (900^0C), whereas HNCS71 showed a broad diffraction peak at 24.9^0 and 43.1^0 (2θ) which corresponds to the graphitic (002) and (101) hexagonal carbon structure[14]. XRD results further confirms that the oxide and metal core was removed from the products but a small amount of iron still present in the carbon which was clearly observed by STEM mapping analysis (Fig S5, ESI†).

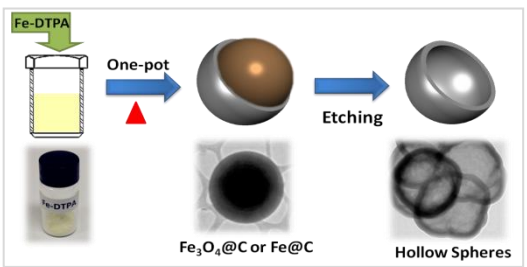

Scheme 1 Pictorial representation of the fabrication of hollow nitrogen-doped carbon spheres.

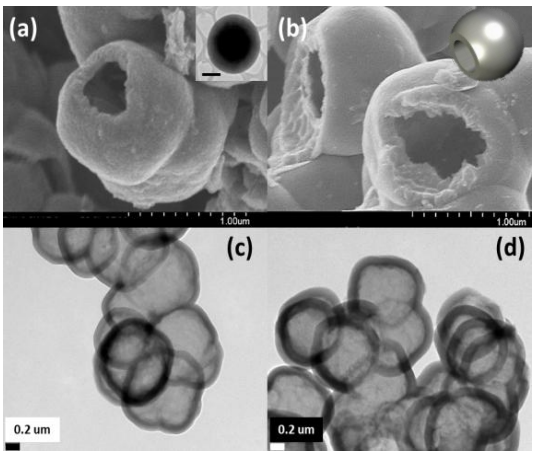

Fig. 1 FFSEM images of (a) HNCS71, (b) HNCS91, and TEM images of (c) HNCS71, (d) HNCS91.; insets in (a) shows a TEM image of a sphere before acid etching (scale bar : 1µm), (b) shows a model of open hollow sphere.

Fig. 2b shows the Raman spectra of HNCS71 and HNCS91 samples exhibit two Raman bands centred at ~1360 and ~1590 cm^{-1}, commonly identified as D- and G-bands of carbon. The D- and G-bands are ascribed to the disorder carbon (sp^3) and ordered graphitic carbon (sp^2), respectively. The nature of carbon present in HNCSs can be identified by taking the ratio of integrated intensity D- and G-bands (I_D/I_G)[15]. A near zero value of I_D/I_G indicates high crystallinity (well graphitized) while near one indicates existence of highly defects in the carbon framework. The I_D/I_G ratio of HNCS71 and HNCS91 were 0.94 and 0.35, respectively. These values suggest that the HNCS91 sample exhibits ordered graphitic carbon than HNCS71, which comes from the higher temperature during the synthesis of precursor and in good agreement with XRD results.

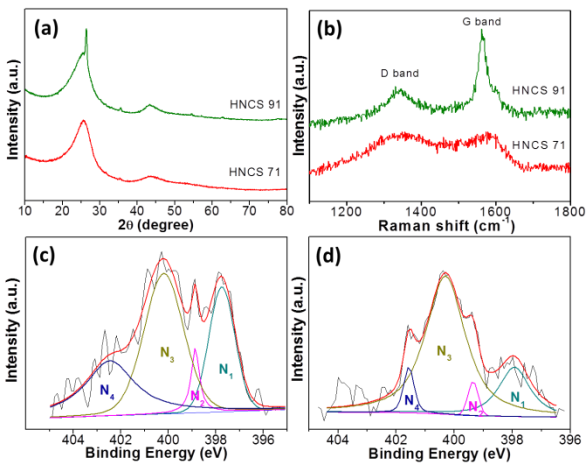

Fig. 2(a) XRD pattern, (b) Raman spectra of HNCSs, XPS N1s spectra of (c) HNCS71, and (d) HNCS91.

The Brunauer-Emmett-Teller (BET) surface area of the HNCS71 and HNCS91 samples were found to be 11.82 and 10.79 m^2 g^{-1}, respectively. These results indicate that the different pyrolysis temperature has no effect on surface area (Fig S6, ESI†). The XPS survey spectra of the hollow carbon spheres revealed the presence of C, O, and N (Fig S7, ESI†). The surface nitrogen content of HNCS71 and HNCS91 samples measured by XPS were found to be 10.4 and 4.12 at%, respectively (Table S2, ESI†). The XPS high resolution N1s spectra was deconvoluted into four peaks with binding energy (BE) values of 397.9, 399.4, 400.7, and ~402 eV for HNCS71 and HNCS91 which can be assigned to the pyridinic-type[12,16], benzonoid amine (-NH-)[17], pyrolic-type[6,18], graphitic-type and oxidize-type[12,18,19] of nitrogen compounds, respectively (Fig 2c-d). HNCS71 catalyst showed higher pyridinic-type nitrogen (26.51%) content than HNCS91 (15.71 %) catalyst. The pyridinic-nitrogen has an extra electron lone pair, which affects the conjugation of the nitrogen lone pair electrons on the nitrogen and hexagonal carbon π-system, and thus creates active sites for ORR[6,12,18,20]. Further, the quantitative analyses of HNCS samples reveal the ratio of doped-N to C (N/C ratio) of HNCS71 and HNCS91 was found to be 0.13% and 0.05%, respectively. The N/C ratio observed in XPS is well agreement with the results observed by the element analysis (Table S2 & S3 ESI †).

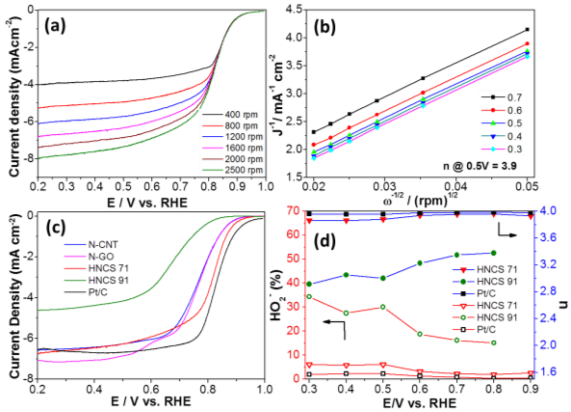

Fig. 3(a) Polarization curves of HNCS71 in O_2-saturated at different rotation speeds, (b) corresponding Koutecky-Levich plots of HNCS71 at different electrode potentials, (c) LSVs of HNCS71, HNCS91, N-CNT, N-GO and Pt/C (10% Pt/C, Johnson Matthew) at 1600 rpm in O_2-saturated 0.1 M KOH, and (d) percentage of peroxide formation and the electron transfer number of these catalyst at different potentials, derived from RRDE experiments.

The electrocatalytic oxygen reduction of hollow nitrogen-doped carbon spheres was studied by rotating disc electrode (RDE) experiments. A set of ORR polarization curves recorded from 400 to 2500 rpm in 0.1M KOH solution at a scan rate 10 mVs^{-1} are displayed in Fig. 3a. The results were compared with a Pt/C catalyst (10%Pt/C, Johnson Matthew). The oxygen reduction onset potentials of HNCS71, HNCS91 and Pt/C catalysts were found to be 0.97, 0.88 and 1.02 V, respectively and the half-wave ($E_{1/2}$) potential was found to be 0.82, 0.69 and 0.85 for of HNCS71, HNCS91 and Pt/C, respectively. The $E_{1/2}$ of HNCS71 is 30 mV lower than a Pt/C catalyst and 130 mV higher than HNCS91 catalyst (Fig.3c). In addition, HNCS71 catalyst showed a good diffusion-limited current suggesting better oxygen reduction activity. A well-defined diffusion-limited current density region of 0.3-0.7 V vs. RHE in RDE at different rotating speeds was used to calculate the number of electrons transferred during the ORR. For comparison, the ORR activity of various carbons was carried out and results were listed in Table S1. The HNCS71 catalyst showed the higher half-wave potential compared with nitrogen-doped graphene and nitrogen-doped carbon nanotube, suggesting HNCS71 electrode can be a potential catalyst for ORR in aq. 0.1 M KOH solution (Fig.3c). The Koutecky-Levich (K-L) plots shown in Fig. 3b are derived from Fig.3a and these plots showed a good linearity and parallelism over all the potential range, which indicates that the electron transfer number for ORR was same even at high potentials[16]. The electrons transfer number (n) of HNCS71 and HNCS91

evaluated at 0.5V vs. RHE was found to be 3.9 and 2.96, respectively, suggesting that HNCS71 electrocatalyst exhibits a dominant four-electron oxygen reduction process. According to these results, HNCS71 exhibits a higher ORR activity than HNCS91, which can be attributed to the higher content of active sites. Especially, HNCS71 catalyst exhibits higher pyridinic-type nitrogen, which is bonded to two carbon atoms in the carbon plane with a lone pair of electrons are associated with the formation of active sites Fe-N_x in carbon framework, and enhance the ORR activity[13,20]. It also consistent with N/C ratio from the element analysis and XPS results (Table S2 & S3, ESI†), revealed HNCS71 catalyst exhibits higher total doped-nitrogen content in the carbon network (N/C ratio), which plays an important role in improving the ORR onset and $E_{1/2}$ potential. Dodelet and co-workers proposed metal cations coordinated by pyridinic-nitrogen atoms at defects of carbon as active ORR sites[13, 20]. To further confirm the ORR results obtained from RDE, we carried out the rotating-ring disk electrode (RRDE) measurements to evaluate the formation of peroxide species (HO_2^-) during the ORR process. The ring and disk currents recorded at 1600 rpm in 0.1M KOH with O_2-saturated over HNCS71, HNCS91 and Pt/C catalysts are shown in Fig. S8, ESI†, it should be mentioned that the ring and disk currents of HNCS71 are almost comparable with the currents observed for a commercial Pt/C catalyst. The percentage of HO_2^- and the number of electron transferred (n) derived from RRDE experiments are presented in Fig.3d. The percentage of peroxide (HO_2^-) formation for HNCS71 catalyst was below 6% over a potential range of 0.3-0.9 V, whereas HNCS91 catalyst produces large amount of peroxide 20-35% over the potential range of 0.3-0.8 V. The electron transfer number was observed to be 3.9 for HNCS71 and about 2.8-3.3 for HNCS91, which is in good agreement with the electron transfer number observed from RDE experiments, it clearly illustrated that HNCS71 catalyst can efficiently reduce oxygen via a 4-electron reduction pathway in alkaline medium.

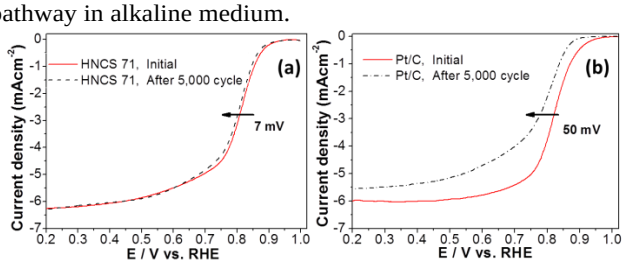

Fig.4. Polarization curves measured during cycling durability tests at 1600 rpm in O_2-saturated 0.1 M KOH (cycling tests were carried out in a potential window of 0.6-1.0V vs. RHE with 50mV s^{-1}).

The electrochemical stability of non-precious catalyst was carried out by performing repeated potentio dynamic cycling durability test for 5,000 cycles in O_2-saturated 0.1M KOH solution with a potential window of 0.6-1.0 V, at a scan rate of 50 mV s^{-1}. It was found that, after 5,000 cycles, a 7 mV negative shift of $E_{1/2}$ was observed for HNCS71, whereas 50 mV negative shifts was observed for Pt/C catalyst (Fig. 4). Further, no change upon cycling on current density of HNCS71 indicated that surface property still maintained during potential cycling test[18,21,22]. On the basis of these studies, HNCS71 catalyst showed better electrochemical stability than Pt/C catalyst.

Conclusions

In summary, we have successfully fabricated a new kind of non-precious catalyst, hollow nitrogen-doped carbon sphere as a cathode catalyst through a simple and scalable approach. The HNCS71 catalyst exhibited comparable ORR activity with that of a commercial Pt/C catalyst and better stability in an alkaline medium. These results demonstrate that the type of nitrogen-doping and tuning the nitrogen content on the carbon framework could be a potential choice for the development of low-cost, highly active ORR catalyst for fuel cell applications.

Acknowledgement

This work was financially supported by DGIST R&D Program of the Ministry of Education, Science and Technology of Korea (14-BD-01).

Notes and references

[a] Department of Energy Systems Engineering, Daegu Gyeongbuk Institute of Science and Technology (DGIST), Daegu, 711-873, Republic of Korea.
[b]State Key Laboratory of Metal Matrix Composites, School of Material Science and Engineering, Shanghai JiaoTong University, Shanghai, 200240 PR China. * E-mail:sangarajus@dgist.ac.kr (S.S); hangtao@sjtu.edu.cn (T.H)
† Electronic Supplementary Information (ESI) available: Experimental details, additional SEM images, additional result. See DOI: 10.1039/c000000x/

1. M. K. Debe, *Nature*, 2012, **486**, 43–51.
2. C.-L. Sun, L.-C. Chen, M.-C. Su, L.-S. Hong, O. Chyan, C.-Y. Hsu, K.-H. Chen, T.-F. Chang, and L. Chang, *Chem. Mater*. **2005**, *17*, 3749.
3. H. A. Gasteiger and N. M. Marković, *Science.*, 2009, **324**, 48–49.
4. F. Jaouen, E. Proietti, M. Lefèvre, R. Chenitz, J.-P. Dodelet, G. Wu, H. T. Chung, C. M. Johnston, and P. Zelenay, *Energy Environ. Sci.*, 2011, **4**, 114–130.
5. Z. Chen, D. Higgins, A. Yu, L. Zhang, and J. Zhang, *Energy Environ. Sci.*, 2011, **4**, 3167–3192.
6. H. T. Chung, J. H. Won, and P. Zelenay, *Nat. Commun.*, 2013, **4**, 1–5.
7. K. Gong, F. Du, Z. Xia, M. Durstock, and L. Dai, *Science.*, 2009, **323**, 760–764.
8. I. Kruusenberg, L. Matisen, Q. Shah, A. M. Kannan, and K. Tammeveski, *Int. J. Hydrogen Energy*, 2012, **37**, 4406–4412.
9. T. Maiyalagan and B. Viswanathan, *Mater. Chem. Phys*. 2005, **93**, 291.
10. W. Yang, T.-P. Fellinger, and M. Antonietti, *J. Am. Chem. Soc.*, 2011, **133**, 206–209.
11. L. Qu, Y. Liu, J.-B. Baek, and L. Dai, *ACS Nano*, 2010, **4**, 1321–1326.
12. H. Peng, Z. Mo, S. Liao, H. Liang, L. Yang, F. Luo, H. Song, Y. Zhong, and B. Zhang, *Sci. Rep.*, 2013, **3**, 1–7.
13. E. Proietti, F. Jaouen, M. Lefèvre, N. Larouche, J. Tian, J. Herranz, and J.-P. Dodelet, *Nat. Commun.*, 2011, **2**, 1–9.
14. H. Jin, H. Zhang, H. Zhong, and J. Zhang, *Energy Environ. Sci.*, 2011, **4**, 3389–3394.
15. X.-Y. Yan, X.-L. Tong, Y.-F. Zhang, X.-D. Han, Y.-Y. Wang, G.-Q. Jin, Y. Qin, and X.-Y. Guo, *Chem. Commun.*, 2012, **48**, 1892–1894.
16. S. Shanmugam and T. Osaka, *Chem. Commun.*, 2011, **47**, 4463–4465.
17. F. G. S. Jr, P. Richa, A. De Siervo, G. E. Oliveira, C. Pinto, and C. H. M. Rodrigues, *Macromol. Mater. Eng.*, 2008, **239**, 675–683.
18. C. V. Rao, C. R. Cabrera, and Y. Ishikawa, *J. Phys. Chem. Lett.*, 2010, **1**, 2622–2627.
19. D. Choudhury, B. Das, D. D. Sarma, and C. N. R. Rao, *Chem. Phys. Lett.*, 2010, **497**, 66–69.
20. M. Lefèvre, E. Proietti, F. Jaouen, and J.-P. Dodelet, *Science.*, 2009, **324**, 71–74.
21. Y. Li, W. Zhou, H. Wang, L. Xie, Y. Liang, F. Wei, J.-C. Idrobo, S. J. Pennycook, and H. Dai, *Nat. Nanotechnol.*, 2012, **7**, 394–400.
22. G. Wu, K. L. More, C. M. Johnston, and P. Zelenay, *Science.*, 2011, **332**, 443–447.